Reference:
Gutiérrez-Sánchez, O., de Mot, B., Daems, N., Bulut, M., Vaes, J., Pant, D. and Breugelmans, T., 2022. Electrochemical Conversion of CO_2 from Direct Air Capture Solutions. **Energy & Fuels**. 36 (21), 13115–13123.

ISSN 1520-5029 (2022), Copyright © 2022 American Chemical Society. All rights reserved
Full text (Publisher's DOI): https://doi.org/10.1021/acs.energyfuels.2c02623
Received 05 August 2022; Received in revised form 11 October 2022; Accepted 20 October 2022

Electrochemical Conversion of CO_2 from Direct Air Capture Solutions

Oriol Gutiérrez-Sánchez[a,b], Bert de Mot[a], Nick Daems[a], Metin Bulut[b], Jan Vaes[b,d], Deepak Pant[b,c], and Tom Breugelmans[*a,c]

[a.] University of Antwerp, Research Group Applied Electrochemistry and Catalysis (ELCAT), Universiteitsplein 1, 2610 Wilrijk, Belgium.

[b.] Separation and Conversion Technology, Flemish Institute for Technological Research (VITO), Boeretang 200, Mol 2400, Belgium.

[c.] Centre for Advanced Process Technology for Urban Resource Recovery (CAPTURE), Frieda Saeysstraat 1, 9052 Zwijnaarde, Belgium

[d.] Department of Solid-state Sciences, Ghent University, Krijgslaan 281/S1, 9000 Ghent, Belgium

* Corresponding author: tom.breugelmans@uantwerpen.be

Abstract

Integrating the alkaline capture of CO_2 from the air with the electrochemical conversion of the obtained (bi)carbonate solution is among the most promising strategies in Carbon Capture & Utilization (CCU) technologies. Thus far this approach has received little or no attention because of the challenging conversion of CO_2 from bicarbonate solutions owing to the parasitic hydrogen evolution reaction (HER). Very recently, thanks to the advances in reactor design and the understanding of the mechanism of bicarbonate electrolysis, promising results were obtained in terms of performance (i.e., >60% FE towards formate or CO at >50 mA cm^{-2}) and as such provided us with the required knowhow to for the first time, construct and validate a proof-of-concept experimental setup where the CO_2 is captured from the air, in the form of a (bi)carbonate solution, through Direct Air Capture and then converted to formate and CO in a zero-gap flow electrolyzer. The presented results provide a new opportunity for upscaling the electrochemical conversion of CO_2, since integrating the capture and the conversion steps is a crucial step to enhance the economic feasibility of the CCU

technology (energy-intensive CO_2 separation can be avoided) and thus increase its chances of industrial implementation.

Keywords

Direct Air Capture, electrochemical CO_2 reduction, bicarbonate electrolysis, Carbon Capture & Utilization

Synopsis

Capturing CO_2 from the air and directly converting it to useful products allows an efficient carbon-neutral strategy to reduce emissions.

Introduction

The rise of the levels of CO_2 in the atmosphere (currently over 400 ppm) is posing a threat to the safety of society as it is one of the main responsible causes for global warming and the rise of temperature worldwide.[1–3] This CO_2 mostly comes from human sources such as industrial waste, energy production or fuel transportation.[4,5] Reducing the amount of CO_2 present in the atmosphere is thus crucial to reduce this effect and, eventually, even revert it.[6] Decreasing the emissions and the production of CO_2 is the most straightforward strategy to reduce the atmospheric CO_2 content however, although several climate laws and global commitments have been set during the last decade, the levels of CO_2 in the air are far from being reduced and are still increasing.[7,8] For this reason, capturing the CO_2 directly from the air (Direct Air Capture, DAC) or industrial waste/point sources have been proposed as one of the main engineered strategies to tackle the problem.[9–11] A typical DAC concept involves a ventilator system which directs the air at a certain flow through a membrane contactor, where it reacts with the capture solution that is flushed in.[12] Nevertheless, due to the low absolute concentration of CO_2 in the air, capturing it is cumbersome and very energy-intensive as such making the process economically unfeasible from an industrial point of view at least with the currently available technology.[13] The main reason is the high energy requirement of recovering back the CO_2. The capture solution, an alkaline solution such as KOH, is converted to carbonate after reacting with CO_2.[14] To separate the carbonate from the rest of the aqueous solution, a regeneration step is performed, consisting of precipitating the carbonate and afterwards calcinating it to extract the gaseous CO_2. The CO_2 is then

compressed and stored. The regeneration and compression steps are high energy-intensive steps, requiring >70% of the overall energy required to capture CO_2.[12] For this reason, it is crucial to find a use for the captured CO_2 preferably as a chemical building block in an industrial process to valorise any potential technology and compensate the high costs of capturing CO_2.[15]

In this respect, several strategies are being investigated within the frame of Carbon Capture and Utilization (CCU) technologies to also valorise the CO_2 and not only capture it. One of the most promising approaches is the electrochemical CO_2 reduction (eCO_2R).[16–19] By the use of renewable energy, an electrocatalyst and an electrochemical cell (or electrolyzer), the CO_2 can be converted to different carbon products such as formic acid, CO, methanol, methane or C_2 products, with the electrocatalyst being the main agent determining the reaction product.[20,21] Currently, most of the research done on eCO_2R is based on supplying pure CO_2 gas to the electrolyzer either as a gas inlet by using Gas Diffusion Electrodes (GDE) or by saturation of the electrolyte before reaction.[22,23] Faradaic Efficiencies (FE) over 90% towards formic acid or CO have been achieved so far when using flow electrolysers and promising results on high-value products such as methanol have also been reported, thus showing the feasibility of converting CO_2 electrochemically to chemical building blocks.[24–26] Nevertheless, delivering pure CO_2 gas to the electrochemical cell requires that the captured CO_2 is regenerated and then compressed, as mentioned above, and thus makes the CCU technology hardly efficient.[27] Instead of pure, gaseous CO_2, using a CO_2-captured solution in form of aqueous (bi)carbonate solution directly as the substrate for the eCO_2R avoids these cumbersome steps and promotes the feasibility of the process.[28–30] In this technology, the post-capture solution is used as an electrolyte and the CO_2 is electrochemically reduced not as a (dissolved) gas, but in the form of (bi)carbonate anion. An efficient method to convert electrochemically bicarbonate is thus crucial to properly integrate the capture and conversion steps. Unfortunately, bicarbonate electrolysis was initially very inefficient in terms of FE and partial current density (CD) in comparison with the analogous gaseous CO_2 electrolysis, mostly due to the proton donor ability of bicarbonate which promotes to a great extent the competing Hydrogen Evolution Reaction (HER).[31–33] In the meantime, extensive research in our group and throughout the scientific community has changed this and the process has become much more efficient as detailed in the following paragraph.

Although direct electrochemical conversion of the bicarbonate anion has been reported, it has been a topic of discussion within the community whether bicarbonate was the substrate of the electrochemical reaction or solely played the role of carbon donor by providing CO_2 (derived from the equilibrium with water) to the surface of the electrode (or both).[34,35] Albeit neither confirming nor discarding any line of thought, several more recent studies showed how promoting the release of CO_2 from bicarbonate in-situ the electrolyzer improved to a great extent both the FE and partial CD of the bicarbonate electrolysis.[36–39] It was found that this release could be promoted by using a Bipolar Membrane (BPM) in combination with a zero-gap flow electrolyzer. Indeed, experimental results demonstrated that bicarbonate is more efficiently converted to CO_2 thanks to the water dissociation occurring in the BPM once the potential is applied (H^+ is released towards the catholyte (1) and OH^- is released towards the anolyte (2)).[40] Due to the zero-gap configuration, the CO_2 is generated close to the surface of the cathode, where it is readily reduced to carbon products (3).[29] Through this strategy, Li *et al.* converted CO_2 from a 3 M bicarbonate solution at 100 mA cm^{-2} obtaining a FE of 64 % and 37% towards formate and CO, respectively.[36–38] However, due to the three-membrane configuration of the BPM (cation exchange, interface and anion exchange layer), a higher Ohmic drop than typical anion- or cation-exchange membranes is observed, thereby increasing to a great extent the cell voltage needed to apply the desired current density and thus lowering the energy efficiency.[40,41] For instance, in our previous study, we observed how, although an FE over 35% towards formate was obtained, the cell voltage was 6.4 V at 400 mA cm^{-2}, which significantly decreased the energy efficiency of the system.[39] Nevertheless, at a lower CD such as 50 mA cm^{-2}, higher FE (58%) and lower cell voltage (3.5 V) were obtained (Figure S1), thus increasing the feasibility of the technology (although further optimization is still needed).

$$H_2O \rightleftarrows H^+ + OH^- \quad (1)$$

$$HCO_3^- + H^+ \rightleftarrows CO_2 + H_2O \quad (2)$$

$$CO_2 + H_2O + 2e^- \rightarrow CO + 2OH^- \quad (3)$$

Using these recent studies, a procedure to electrolyze bicarbonate solutions was benchmarked and thus warranting the potential of electrolyzing CO_2 post-capture solutions.

In this study, we report for the first time, the electrochemical conversion of CO_2 that has been obtained directly from the air, integrating both the capture and the conversion steps in one single proof-of-concept carbon capture and conversion system. By capturing the CO_2 from the air in the form of (bi)carbonate with a DAC system and then electrolyzing the (bi)carbonate solution in a zero-gap flow electrolyzer, CO_2 was converted to formate and CO by using a SnO_2-based and an Ag-based electrocatalyst, respectively. The aim of this study is to benchmark the first step towards implementing this ambitious, but elegant concept that is the integration of the capture and conversion steps within CCU. With the results shown in this paper, we have materialized, by giving experimental proof, those perspectives and assessments (i.e., Sullivan et al., 2022, Li et al., 2022 and Gutierrez-Sanchez et al., 2022) that proposed the integrated approach as one of the most promising strategies to close the CO_2 cycle with a positive techno-economic balance.

1 Experimental method

1.1 Materials and solutions

All the chemicals were obtained from commercial sources and used without purification unless stated otherwise. The capture solution and the anolyte were prepared by dissolving the corresponding amount of 1 M of potassium hydroxide pellets (Chem-Lab) in Ultra-Pure water (MilliQ, 18.2 MΩ cm). The capillary module 3M™ Liqui-Cel™ MM-1.7x8.75 (Figure S2) was chosen as a membrane contactor for CO_2 sequestration based on a previous evaluation performed at VITO. Tin (IV) oxide nanopowder (<100 nm, >99%) and Ag nanopowder (<100 nm, >99.5%) from Sigma-Aldrich were used as the electrocatalyst and porous carbon paper AvCarb MGL 190 (Fuel Cell Store) was used as catalyst support. For the counter electrode, Ni foam (Nanografi) was used. To separate the catholyte and the anolyte, a Bipolar Membrane (FumaSep) was used.

1.2 Direct Air Capture: Setup assembly and procedure

The capillary module is charged into the bench-scale setup and contained in a tailor-made module holder (Figure 1). The module housing was cut on two sides to allow free air movement through the capture module (in vertical position) in and out, perpendicular to the capillaries' direction. The 1 M KOH capture solution is pumped through the valve at 75 mL

min^{-1}, towards the inside (lumen side) of the capillaries. In the capillary module, the membrane contactor allows enhanced CO_2 transport from the atmospheric air to the capture solution.[42] The fan is set to an operational airflow velocity of 0.22 m s^{-1}. The channel displaces a volumetric flow of ~12 m³ h^{-1} air (fan system's exit area = 180 cm²) to the module holder, which corresponds to a CO_2 flow of ~0.2 mol h^{-1}. The airflow that exits the fan system goes through a stack of tubes, to obtain a laminar flow. After the module holder, an exit channel is foreseen to avoid shape turbulence. The purpose of such design is to avoid pressure drops, in addition to the resistance from the tested module and capillaries. To avoid water losses due to evaporation, adequate humidification was integrated into the capture system to avoid/minimize this effect, making water compensation in the KOH solution vessel unnecessary. The pH of the solution is monitored and registered to evaluate the evolution of the acidity of the solution. The experiment is stopped after 8.5 hours of duration and the solution is stored. The solutions were sealed and remained stable for several weeks (pH invariant at ~10.6). After the capture experiment, a mixture of carbonate and bicarbonate anion is expected in the solution. The exact concentration of the species and the ratio is determined as described in section 1.5.1.

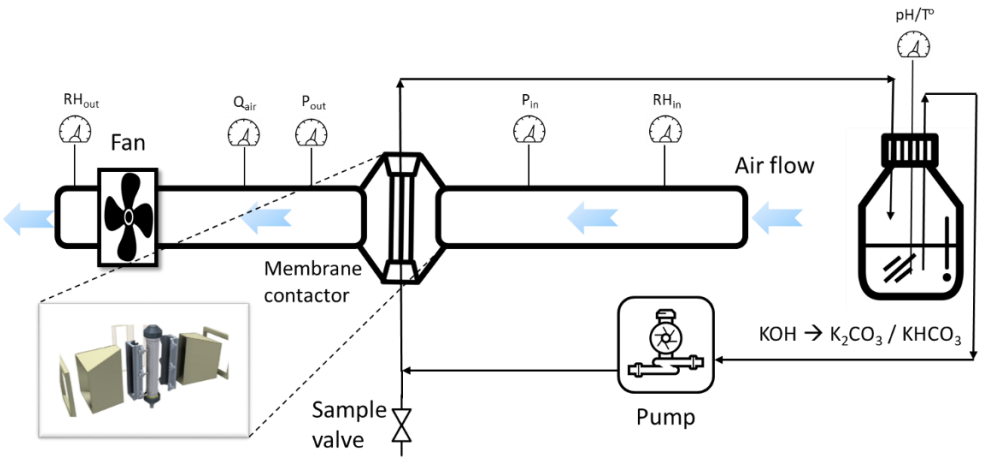

Figure 1: Bench scale and schematic CO_2 capture test setup. It consists of a fan system and channel that guides the airflow to a central module holder, followed by an exit channel. The test module holder is located at the center of the bench-scale setup, through which the capture solution flows. The module is adapted such that it can be placed vertically and receive airflow.

1.3 Working electrode manufacturing

Working electrodes for electrolysis were manufactured by spray coating a catalyst ink (SnO_2 or Ag nanoparticles) on top of a 4x4 cm porous carbon paper following the procedure described in our previous study and inspired by the electrode optimization study of Lees *et al*.[38,43] In those studies, it was shown how, to maximize the performance of the catalyst in terms of FE and partial CD, the microporous layer, the binder and the PTFE layer had to be avoided in the manufacturing the working electrode. It is assumed that the stability of the catalyst is affected by the lack of binder, however, in this study, we did not evaluate the stability of the system.[44] Every electrode used in the experiments had a final loading of 2.0 ± 0.2 mg cm^{-2} of nanoparticles. The resulting electrode SnO_2/C was used to convert the DAC solution to formate ($HCOO^-$) while Ag/C was used to convert the DAC solution to CO in separated experiments.

1.4 (Bi)carbonate electrolysis: setup and procedure

The electrochemical experiments were performed in a custom build zero-gap flow electrolyzer (Figure 2). The same electrolyzer was used in our previous studies, where the details on the configuration are found.[40,45] The (bi)carbonate solution obtained from DAC was used as the catholyte. The catholyte enters the electrolyzer from the bottom, where it flows through the interdigitated designed graphite flow channel pressed against the working electrode to the top of the electrolyzer thereby optimizing the mass transfer of the electrolyte towards the catalyst surface. On the other side, on top of the electrode, the BPM is placed. The zero-gap configuration allows the membrane and the cathode to be pressed to each other, promoting the protonation of the (bi)carbonate species next to the electrode, where CO_2 is reduced to products. The anodic compartment of the electrolyzer is like the previously described cathode side. However, here a nickel foam was used as an electrode and 1 M KOH as an anolyte. The electrolyzer was connected to an Autolab potentiostat (model PGSTAT302N).

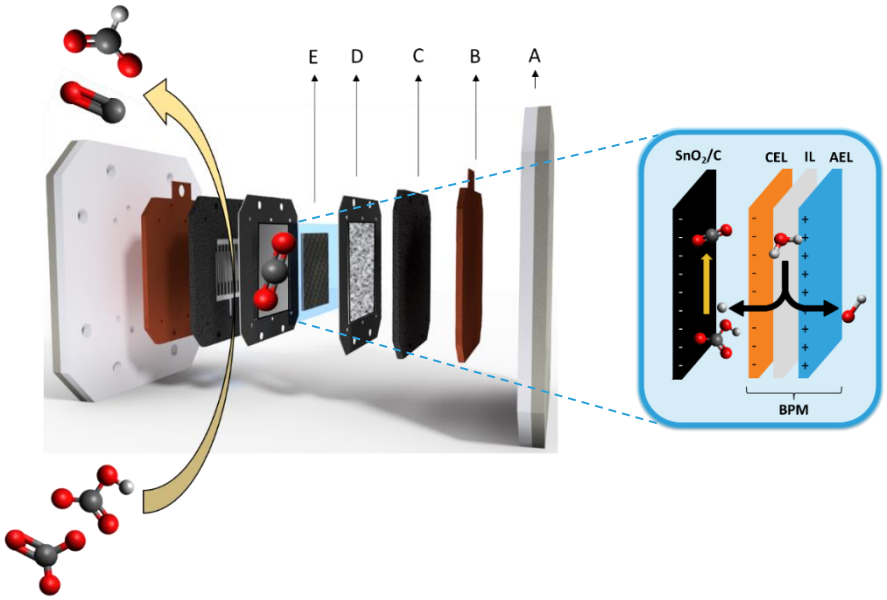

Figure 2: Schematic representation of the (bi)carbonate zero-gap flow electrolyzer involving a BPM used in this study. Components description: A) end-plates; B) copper current collectors; C) interdigitated flow channel; D) Catalysts gaskets; E) BPM.

The experimental conditions were set based on the optimization study for bicarbonate electrolysis performed recently by our group.[43] From this study, the most optimal flow rate, temperature and CD to achieve the highest energy efficiency were chosen. The DAC solution was fed in single-pass mode to the cathode side of the electrolyzer using a High-Performance Liquid Chromatography (HPLC) pump which allowed for accurate control of the flow rate at 5 mL min^{-1}. On the anode side, a peristaltic pump was used to recirculate the 1 L of anolyte at a flow rate of 20 mL min^{-1}. The complete electrolyzer was placed in an oven (Binder Oven) to fix the temperature of the system at 25 °C. Chrono-potentiometric experiments were performed at 50 mA cm^{-2}. For liquid analysis (formate), samples were taken and stored after 30 minutes, while for gas analysis (CO), online analysis was performed (see section 1.5.2).

1.5 Product analysis and characterization

1.5.1 Characterization of DAC solutions

After capturing CO_2 for 8.5 hours and reaching equilibrium, the DAC solution is a mixture of dissolved CO_2, bicarbonate and carbonate, together known as Dissolved Inorganic Carbon (DIC). By measuring the final pH and using the corresponding equilibrium equations and the total concentration of DIC present in the solution, the concentration of each specie

(carbonate, bicarbonate and dissolved CO_2) is obtained (Equation S1). We can assume a negligible concentration of dissolved CO_2 (<0.01%) at the working pH range (14-10). At the final pH obtained in this study (~10.6), since the carbonate/bicarbonate half-neutralization point is surpassed and thus the initial KOH was already converted to carbonate, the total DIC is equal to the concentration of KOH used as capturing solution (1 M). However, for this study, we could not make this assumption. As we disassembled the capture setup after the experiment, we observed (bi)carbonate salt precipitation around the capillary structure of the membrane contactor (Figure S3). Therefore, alkalinity is lost during the capture experiment and thus the concentration of DIC is lower than the initial concentration of KOH (although the ratio of bicarbonate/carbonate is maintained as it only depends on the pH). Even for upscaled and optimized DAC setups, we believe other methods must be used to properly quantify the (bi)carbonate species in DAC solutions since there will always be a loss of alkalinity to a certain extent due to the pH and concentration gradients in the contactor-solution interface. For this reason, in this study, a procedure to properly characterize DAC solutions for the integrated capture and conversion of CO_2 was set up. We chose Fourier Transformed Infrared Spectroscopy (FT-IR) as the technique to characterize (bi)carbonate solutions. The choice is two-folded: FT-IR has been previously used for instance by Joshi *et al.* to quantify bicarbonate and carbonate in solid mixtures and by Baldassarre *et al*. to measure the pH using (bi)carbonate systems.[46,47] We can then use FT-IR to quantify bicarbonate and carbonate in aqueous solutions and then use the pH ratio calculated with the equilibrium equations as a validation of the method.

The trigonal planar carbonate anion (CO_3^{2-}) has symmetry D_{3h} and their vibrational modes v_2 (A_2''), v_1 (A_1') and v_3 (E') are active in the infrared (IR) spectra. Bicarbonate (HCO_3^-) has symmetry C_{2v} and, in addition to the modified CO_3 modes, the vibrational modes corresponding to the presence of OH v_5 (A'), v_4 (A') and v_1 (A') are also active in the IR spectra, (Table S1).[48] To quantify the concentration of each specie present in the DAC solutions, we calibrated the absorption peak v_3 (E') found at 1380 cm^{-1}, corresponding to carbonate, and the absorption peak v_2 (A') found at 1620 cm^{-1}, corresponding to bicarbonate, with different bicarbonate/carbonate buffer solutions (Figure S4). The carbonate peak v_3 (E') was corrected by subtracting the contribution of the bicarbonate's vibrational mode v_2 (A') using the absorbance correction method. As a result, FT-IR could be used on the DAC solutions to obtain

the real concentration of bicarbonate and carbonate in the solution through interpolation of the absorption peaks found at 1380 and 1620 cm^{-1} to the calibration slope.

As a validation of the characterization technique, a similar bicarbonate/carbonate ratio was obtained either by calculating it with the pH (33%/67% ± 4%) or with FT-IR (25%/75% ± 8%). The concentration of DIC, carbonate and bicarbonate are given as an average of three independent DAC experiments. As mentioned, the relative abundance of dissolved CO_2 is negligible (<0.01%) at the pH range of the study and therefore not considered as part of the DIC. The error bars correspond to the standard deviation. Thermo Scientific spectrometer (model Nicolet iS10) was used to characterize the DAC solutions with FT-IR. The DAC solutions were not previously treated.

1.5.2 (Bi)carbonate electrolysis product analysis

For liquid product analysis, Agilent 1200 High-Performance Liquid Chromatography with an Agilent Hi-Plex H 7.7×300 mm column was used to separate the product and an Agilent 1260 RID detector to detect and quantify formate in the form of formic acid. The samples were previously diluted with water and acidified with H_2SO_4 to avoid bubble formation and obstruction in the column. H_2SO_4 0.01 M was used as the mobile phase. For electrolysis experiments using SnO_2/C as an electrocatalyst, only formate was analysed as a product since the selectivity of the reaction falls outside the scope of this study. Other co-products (mainly H_2 and in a much lesser amount CO) were not quantified.

For gas product analysis, Shimadzu 2014 Gas Chromatography with ShinCarbon St 100/120 2mx1mm column (Restek, USA) installed was used. Helium gas (10 ml min^{-1}) was used as the carrier, and the column temperature was set at 40 °C for 180 s. After the initial stage, the column's temperature was raised from 40 °C min^{-1} to 250 °C. Detection of CO was done by a thermal conductivity detector at 280 °C. For electrolysis experiments using Ag/C as an electrocatalyst, only CO was analysed as a product.

The results are presented in the form of FE (Equation S2) and Cell Voltage and compared to literature results corresponding to electrolysis experiments of bicarbonate solutions at different concentrations. The results are presented as an average of two independent experiments and the error bars correspond to the standard deviation.

2 Results and discussion

2.1 (Bi)carbonate solution obtained from Direct Air Capture

When the atmospheric CO_2 passed through the vessels of the membrane contactor, it reacted with the KOH of the capture solution forming $KHCO_3$ (4). As KOH was consumed, the alkalinity of the capture solution diminished and thus the pH decreased gradually. The $KHCO_3$ further reacted to form K_2CO_3 until the KOH was exhausted (5). Afterwards, CO_2 acidified water, which protonated the K_2CO_3 to form $KHCO_3$ (6). In Figure 3, where the evolution of the pH over time (blue) for the DAC experiments is displayed, these processes can be observed. During the first four hours of the experiment, the pH decreased gradually from 13.8 to 13.1 due to the consumption of OH^-. Until this point, the $[K_2CO_3] > [KHCO_3]$. Then, from the fourth to the fifth hour, the half-neutralization point was reached ($[K_2CO_3] = [KHCO_3]$), resulting in an abrupt decrease of the pH from 13.1 to 10.9. From the fifth hour until the end of the experiment (8.5 h), the $[K_2CO_3] < [KHCO_3]$ and the pH continued decreasing from 10.9 to 10.4 due to the acidification of the solution. Long-term capture experiments showed how, after 8.5 h, the pH barely decreased. In fact, from 8.5 to 72 h, the pH decreased from 10.4 to 9.9 (Figure S5). We attribute this result to the strong buffering effect of the carbonate/bicarbonate solution (the theoretical concentration of DIC at this point is 1 M based on equilibrium equations), stabilizing the pH and thus making the capture of CO_2 harder. This could be solved by, for instance, increasing the membrane-solution contact surface larger (more CO_2 is in contact with the capture solution). Therefore, the experiments were stopped at 8.5 h. The obtained post-capture solution was a mixture of K_2CO_3 and $KHCO_3$, referred to as (bi)carbonate solution. The ratio of the mixture was determined by the final pH (10.6 after reaching equilibrium) and the equilibrium equations of carbonic acid in aqueous media (Equations S1). At pH 10.6, the bicarbonate/carbonate calculated ratio was 33%/67% ± 4% (Figure 3, orange).

$$CO_2 + KOH \rightleftarrows KHCO_3 \quad (4)$$

$$KHCO_3 + KOH \rightleftarrows K_2CO_3 + H_2O \quad (5)$$

$$K_2CO_3 + CO_2 + H_2O \rightleftarrows 2KHCO_3 \quad (6)$$

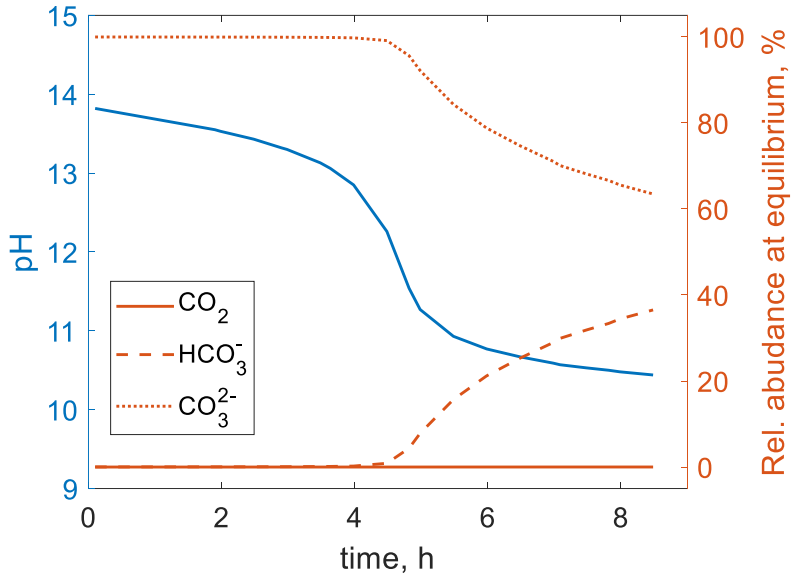

Figure 3: Evolution of the pH over time of a DAC experiment using KOH 1 M as capture solution and air as CO_2 source (blue). Relative abundance of the carbonic species in the DAC solution after reaching equilibrium (orange).

The concentration of bicarbonate and carbonate (and thus DIC) of the DAC solutions were obtained by characterizing the solution with FT-IR. In Figure 4, the IR spectra of the DAC solution (averaged from three independent DAC experiments, Figure S6) are displayed. As observed, both the characteristic absorption peaks of carbonate and bicarbonate selected to quantify the concentration are present. The calculated bicarbonate concentration was 0.166 ± 0.063 M, while the carbonate concentration was 0.492 ± 0.032 M. The concentration distribution corresponded to a bicarbonate/carbonate ratio of 25%/75% ± 8%, which was in the same range as the one calculated from the equilibrium equations, 33%/67% ± 4%. We assumed the slight deviation to shifts in the equilibrium as the solutions were exposed to open air during the manipulation and the characterization of the samples.

The total DIC concentration was 0.658 ± 0.031 M which is in contrast with the initial KOH concentration of 1 M. As we anticipated, there was a loss of alkalinity due to the precipitation of the potassium (bi)carbonate salts, therefore the assumption of [DIC] ≠ $[KOH]_o$ was adequate. Based on the total concentration of DIC measured, approximately, 5.7 g of KOH was lost within the duration of the experiment, corresponding to a loss rate of 0.7 g h^{-1}. It is very important to highlight this observation, as it is crucial for the techno-economic validation of a potential upscaled technology to minimize losses in every step. A huge alkalinity loss rate would require human maintenance more often, increasing the costs of the technology.

Therefore, to minimize this effect, engineering efforts are required both for lab and upscaled levels, which is an interesting pathway to continue the research on this topic. On the other hand, the CO_2 capture efficiency (Equation S3) was 14.8 ± 0.7 %. This capture efficiency allowed us to capture CO_2 with a rate of 1.4 ± 0.7 g h^{-1} and thus obtain a relatively high concentrated (bi)carbonate solution after 8.5 h. However, in long-term capture experiments, we observed that the pH almost did not drop further from 10 after more than 48 h of experiment. We attributed this effect to the loss of alkalinity mentioned earlier and the fact that the DAC solution acts as a buffer (CO_2-bicarbonate-carbonate equilibrium). An increase in the mass transport of CO_2 from the air to the solution by a combination of minimizing the alkalinity loss and increasing the capture efficiency (for instance, by adding capture modules) would allow going lower in the pH, therefore capturing a higher amount of CO_2 and increasing the capture rate.

[HCO_3^-] (M)	0.166 ± 0.063
[CO_3^{2-}] (M)	0.492 ± 0.032
[DIC] (M)	0.658 ± 0.031
Capture rate (g h^{-1})	1.40 ± 0.07
Capture eff. (%)	14.8 ± 0.7

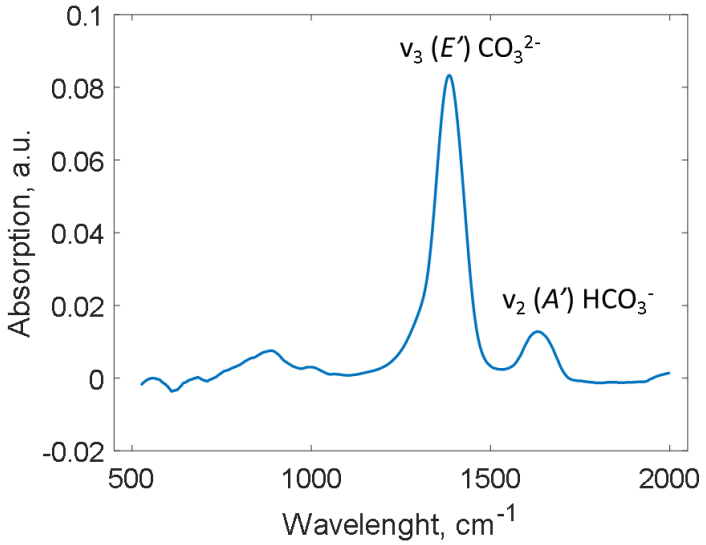

Figure 4: FT-IR spectra of the DAC solution and concentration of each specie, capture rate and capture efficiency calculated based on the data obtained from the FT-IR characterization.

In this section, we have captured CO_2 from the air using a 1 M KOH solution and we have validated FT-IR as a method to characterize DAC solutions. A total DIC concentration of 0.658 ± 0.031 M (0.166 ± 0.063 M of bicarbonate and 0.492 ± 0.032 M carbonate) was obtained. The DAC solutions obtained in the CO_2 capture experiment were mixed and evaluated as a single electrolyte in the following (bi)carbonate electrolysis experiment.

2.2 Electrolysis of the Direct Air Capture solution

As mentioned, the DAC solution was used as such as the catholyte in a zero-gap (bi)carbonate flow electrolyzer. A SnO_2/C catalyst was used to convert DAC to formate and an Ag/C catalyst to convert DAC to CO, in separate experiments. In the past, carbonate and bicarbonate were studied separately as carbon donors for eCO_2R, but a mixture of both has never been studied.[36,49] However, given that the BPM dissociates water acidifying the catholyte, it can be expected that most of the species present on the surface of the electrode were bicarbonate and dissolved CO_2 (from carbonate and bicarbonate, respectively). Its relative abundancies will depend on the protonation rate of the catholyte. For this reason, the performance of the electrolyzer is anticipated to be around or slightly below that of pure bicarbonate electrolytes. Consequently, our results can be compared to the state-of-the-art in bicarbonate electrolysis at different concentrations (1, 2 and 3 M). Our previous work on bicarbonate electrolysis to formate and the work of Li *et al*. on bicarbonate electrolysis to CO were used as references.[36,43] These studies achieved the highest FE ever reported at the CD of study (50 mA cm^{-2}). Additionally, the reactor configuration (zero-gap flow cell and BPM) is similar, differing in some engineering parameters such as the electrode preparation or the size of the reactor. Nevertheless, it allows the early evaluation of how valid of the proposed approach.

The results of electrolyzing the DAC solution towards formate are shown in Figure 5 (left). As observed, for the state-of-the-art there is a clear decreasing trend of the FE with the concentration of $KHCO_3$, which is expected as fewer carbon donor species are present in the solution. For instance, the state-of-the-art's FE is 58, 48 and 38% at 3, 2 and 1 M $KHCO_3$, respectively, meaning that per unit of molarity there is a decrease of 10% FE. In this work, where a 0.658 ± 0.031 M DIC solution was used, the obtained FE was 16%, instead of the 34% that was expected based on the literature observations (corresponding to a 0.658 M $KHCO_3$ solution). It is reasoned that this is a consequence of K_2CO_3 being the major specie (0.492 ± 0.032 M) in the DAC solution, which requires an extra step to release CO_2 for reaction. Indeed, to convert K_2CO_3 to dissolved CO_2, two units of H^+ (dissociated from H_2O in the BPM) were needed, while only one was needed to convert $KHCO_3$ to dissolved CO_2 (Figure 6). In a BPM, certain overpotential is required to dissociate water, which depends on the Point of Zero Charge (PZC) and the configuration of the reactor.[50,51] Therefore, if one or more protons need to be dissociated from water to convert (bi)carbonate to CO_2, this will be reflected in the FE

of the reaction. When K_2CO_3 is in solution, two protons are needed to convert it to CO_2, explaining why lower FE (16%) was achieved with a mixture of K_2CO_3 and $KHCO_3$ when, hypothetically, in pure 0.5 M $KHCO_3$ solutions the FE should be around 34%. On the other hand, the Cell Voltage slightly decreased, following the trend of the state-of-the-art.

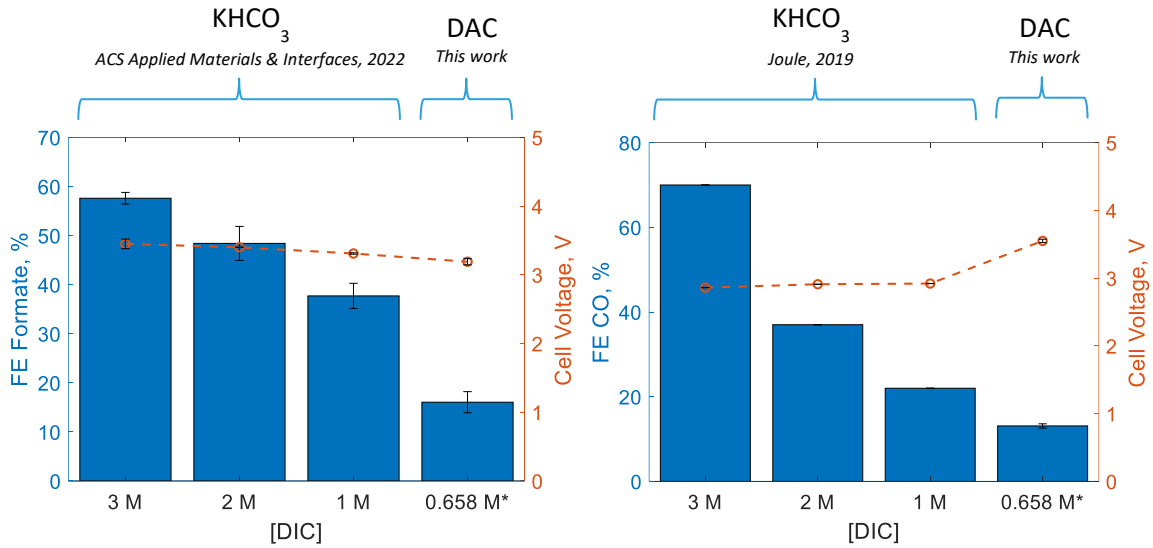

Figure 5: FE towards formate (left) and CO (right) of the electrolysis of a DAC solution of 0.658 ± 0.031 M DIC at 50 mA cm^{-2}. The results are compared to state-of-the-art FE of $KHCO_3$ electrolysis.[36,43]

The results of the electrolysis revealed, for the first time, the possibility to electrochemically convert CO_2, directly from the DAC solutions, towards formate and CO. The electrolysis of the DAC solutions, although constituting a mixture of bicarbonate and carbonate (33%/67%), followed a similar trend to when using 100% $KHCO_3$ solutions in the sense that the FE values decreased with the carbon availability and that they can be converted electrochemically in a zero-gap electrolyzer. Therefore, the know-how on bicarbonate electrolysis can be accurately extrapolated to DAC electrolysis (or to the electrolysis of bicarbonate/carbonate mixtures). Although the conversion of DAC to formate is most interesting from a proof-of-concept point of view in the concept of formate fuel cells, the conversion of DAC to CO is of high interest for the integrated route due to the production of OH^- as a co-product of the eCO_2R which is not occurring during the formation of formate. Indeed, in this case, the alkalinity is regenerated and thus allows recycling of the capture solution for a new round of CO_2 capture from air, thereby closing the cycle. From our point of view, the performance of the direct electrochemical conversion of DAC capture solutions can be further improved by increasing

the carbon loading of said solutions. Indeed, since in bicarbonate electrolysis good FE (>40%) has been obtained at high current densities (>200 mA cm^{-2}) when the concentration of bicarbonate is high (>1 M), this should also be possible with DAC solutions. In conclusion, an improved DAC step is strongly needed to increase the overall efficiency of the CCU technology.

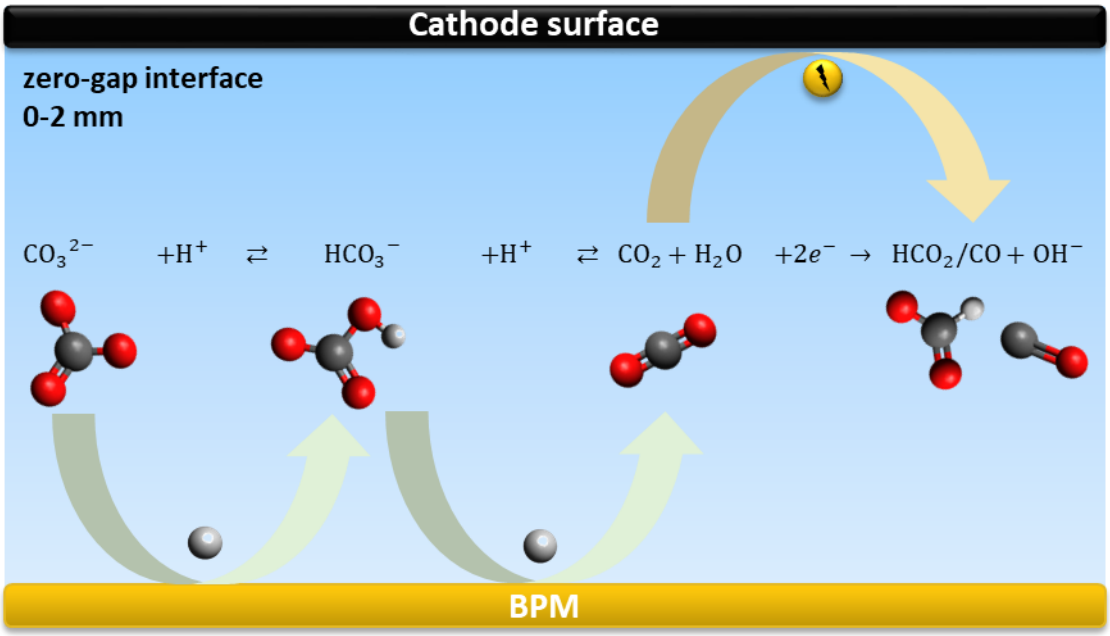

Figure 6: Schematic representation of the reactions happening at the zero-gap electrolyte interface when electrolyzing a DAC solution. Carbonate ions require two protonation steps to deliver CO_2, while only one is needed for bicarbonate ions. The CO_2 is then evolved to products as it is released close to the surface of the electrode.

The results of the experiments using an Ag/C electrocatalyst to convert DAC to CO are shown in Figure 5 (right). The trend of the FE and the concentration of $KHCO_3$ observed previously for bicarbonate electrolysis to formate in the state-of-the-art (decreasing FE with the concentration of $KHCO_3$) was observed here as well. However, in the case of bicarbonate electrolysis to CO, the decrease of the FE with concentration followed a multiplicative inverse trend (1/x) instead of linear, as was the case when formate was produced. For instance, the state-of-the-art FE is 70, 37 and 22% at 3, 2 and 1 M $KHCO_3$, respectively, meaning that the decrease of the FE is approximately halved with each decrease, i.e. it decreased a 33% from 3 to 2 M and 15% from 2 to 1 M. When we electrolyzed the DAC solution, a FE towards CO of

13% was obtained, thus the FE decreased by 9% (approximately halved) compared to using 1 M $KHCO_3$ as electrolyte (from 22 to 13%). For CO production, DAC electrolysis thus follows the same trend as in the state-of-the-art $KHCO_3$ solutions, making us believe both the DAC and the pure $KHCO_3$ electrolytes behave similarly. Therefore, the reasoning followed when formate was the product (the presence of K_2CO_3 decreases the FE trend) is not applicable for CO. For further understanding of this behavior, an independent screening for CO production, this time only using $KHCO_3$ and the same engineering conditions (since the parameters of the state-of-the-art slightly differs) is needed.

3 Conclusions

In this study, we have converted electrochemically the CO_2 that comes directly from the air by electrolyzing a DAC solution in a bicarbonate zero-gap flow electrolyzer. After 8.5 h of capturing CO_2 with a 1 M KOH solution, a mixture solution of (bi)carbonate was obtained. By developing a procedure to characterize DAC solutions with FT-IR, the concentration of each specie and the alkalinity loss were accurately quantified. The DAC solution was directly used as catholyte in the electrolyzer and, by applying 50 mA cm^{-2}, a FE of 16% towards formate (when using a SnO_2/C as electrocatalyst) and 13% towards CO (when using Ag/C) were obtained, showing conversion of atmospheric CO_2 towards industrially relevant carbon products. By comparing the results obtained to state-of-the-art data on $KHCO_3$ electrolysis we observed that the ratio of FE with the concentration of carbon load is maintained (higher FE when the concentration is higher) for DAC solutions, too. Therefore, it is postulated that the concentration of DIC in the DAC solution is crucial to increase the efficiency of the electrochemical conversion step and thus the overall CCU process. Further research should focus on how to capture more CO_2 from KOH solutions. For instance, starting from a higher concentration of KOH would allow capturing more CO_2, although the integrity of the setup, the alkalinity loss and the increased duration of the operational capture time must be considered, too. On the other hand, optimizing the (bi)carbonate electrolyzer could also yield improved performance. High energy losses were observed (high cell voltage) due to the presence of a BPM and progress in this field should thus be considered as well if one is to enhance the system performance. Finally, further integrating both systems, for instance by coupling the electrolyzer directly to the DAC setup, is an interesting future perspective as well, although the separate optimization of both systems should be provided, first. In conclusion,

this proof-of-concept study sets a new benchmark for integrating the capture and the (electrochemical) conversion of CO_2 within the field of CCU.

Supporting information

Formulas and equations, membrane contactor specifications, FT-IR spectra, FT-IR calibration, long-term DAC

Conflicts of interest

There are no conflicts to declare.

Acknowledgements

The authors wish to thank Silvia Vangeel and Bart Molenberghs from VITO for providing the experimental background and know-how of Direct Air Capture and for performing the tests. O.G.S. is supported by a PhD grant from VITO's strategic research funds (project no. 1810257). B.D.M is supported by the University of Antwerp's Strategic Basic Research Industrial Research Fund (BSO-IOF) (project no. FFI170350). This research was also supported by the project CAPTIN (under the Moonshot initiative of VLAIO/Catalisti, Grant number HBC.2019.0076 and HBC.2021.0255).

References

(1) Cavallaro, N., Shrestha, G., Birdsey, R., Mayes, M. A., Najjar, R. G., Reed, S. C., Romero-Lankao, P., Zhu, Z., Eds.; *Second State of the Carbon Cycle Report*; Washington, DC, 2018. https://doi.org/10.7930/Soccr2.2018.

(2) Lüthi, D.; le Floch, M.; Bereiter, B.; Blunier, T.; Barnola, J.-M.; Siegenthaler, U.; Raynaud, D.; Jouzel, J.; Fischer, H.; Kawamura, K.; Stocker, T. F. High-Resolution Carbon Dioxide Concentration Record 650,000–800,000 Years before Present. *Nature* **2008**, *453* (7193), 379–382. https://doi.org/10.1038/nature06949.

(3) Blunden, J.; Boyer, T. State of the Climate in 2020. *Bull Am Meteorol Soc* **2021**, *102* (8), S1–S475. https://doi.org/10.1175/2021BAMSStateoftheClimate.1.

(4) Dietz, T.; Rosa, E. A. Effects of Population and Affluence on CO_2 Emissions. *Proceedings of the National Academy of Sciences* **1997**, *94* (1), 175–179. https://doi.org/10.1073/pnas.94.1.175.

(5) Nagelkerken, I.; Connell, S. D. Global Alteration of Ocean Ecosystem Functioning Due to Increasing Human CO_2 Emissions. *Proceedings of the National Academy of Sciences* **2015**, *112* (43), 13272–13277. https://doi.org/10.1073/pnas.1510856112.

(6) Masson-Delmotte, V.; P. Zhai; H.-O. Pörtner; D. Roberts; J. Skea; P.R. Shukla; A. Pirani; W. Moufouma-Okia; C. Péan; R. Pidcock; S. Connors; J.B.R. Matthews; Y. Chen; X. Zhou; M.I. Gomis; E. Lonnoy; T. Maycock; M. Tignor; T. Waterfield (eds.). *Annex I:Glossary. Global Warming of 1.5°C.*; 2018.

(7) Tollefson, J. The Hard Truths of Climate Change — by the Numbers. *Nature* **2019**, *573* (7774), 324–327. https://doi.org/10.1038/d41586-019-02711-4.

(8) Rogelj, J.; Popp, A.; Calvin, K. v.; Luderer, G.; Emmerling, J.; Gernaat, D.; Fujimori, S.; Strefler, J.; Hasegawa, T.; Marangoni, G.; Krey, V.; Kriegler, E.; Riahi, K.; van Vuuren, D. P.; Doelman, J.; Drouet, L.; Edmonds, J.; Fricko, O.; Harmsen, M.; Havlík, P.; Humpenöder, F.; Stehfest, E.; Tavoni, M. Scenarios towards Limiting Global Mean Temperature Increase below 1.5 °C. *Nat Clim Chang* **2018**, *8* (4), 325–332. https://doi.org/10.1038/s41558-018-0091-3.

(9) Deutz, S.; Bardow, A. Life-Cycle Assessment of an Industrial Direct Air Capture Process Based on Temperature–Vacuum Swing Adsorption. *Nat Energy* **2021**, *6* (2), 203–213. https://doi.org/10.1038/s41560-020-00771-9.

(10) Sara Budinis. *Direct Air Capture*. IEA, Paris. https://www.iea.org/reports/direct-air-capture-2 (accessed 2022-09-20).

(11) Raksajati, A.; Ho, M. T.; Wiley, D. E. Reducing the Cost of CO_2 Capture from Flue Gases Using Aqueous Chemical Absorption. *Ind Eng Chem Res* **2013**, *52* (47), 16887–16901. https://doi.org/10.1021/ie402185h.

(12) Keith, D. W.; Holmes, G.; st. Angelo, D.; Heidel, K. A Process for Capturing CO_2 from the Atmosphere. *Joule* **2018**, *2* (8), 1573–1594. https://doi.org/10.1016/j.joule.2018.05.006.

(13) Craig Bettenhausen. The Life-or-Death Race to Improve Carbon Capture. *Chemical & Engineering News*. 2021, p 99 (26).

(14) Mahmoudkhani, M.; Keith, D. W. Low-Energy Sodium Hydroxide Recovery for CO_2 Capture from Atmospheric Air—Thermodynamic Analysis. *International Journal of Greenhouse Gas Control* **2009**, *3* (4), 376–384. https://doi.org/10.1016/J.IJGGC.2009.02.003.

(15) Artz, J.; Müller, T. E.; Thenert, K.; Kleinekorte, J.; Meys, R.; Sternberg, A.; Bardow, A.; Leitner, W. Sustainable Conversion of Carbon Dioxide: An Integrated Review of Catalysis and Life Cycle Assessment. *Chem Rev* **2018**, *118* (2), 434–504. https://doi.org/10.1021/acs.chemrev.7b00435.

(16) Sánchez, O. G.; Birdja, Y. Y.; Bulut, M.; Vaes, J.; Breugelmans, T.; Pant, D. Recent Advances in Industrial CO_2 Electroreduction. *Curr Opin Green Sustain Chem* **2019**, *16*, 47–56. https://doi.org/10.1016/j.cogsc.2019.01.005.

(17) Durst, J.; Rudnev, A.; Dutta, A.; Fu, Y.; Herranz, J.; Kaliginedi, V.; Kuzume, A.; Permyakova, A. A.; Paratcha, Y.; Broekmann, P.; Schmidt, T. J. Electrochemical CO_2 Reduction – A Critical View on Fundamentals, Materials and Applications. *CHIMIA International Journal for Chemistry* **2015**, *69* (12), 769–776. https://doi.org/10.2533/chimia.2015.769.

(18) Gabrielli, P.; Gazzani, M.; Mazzotti, M. The Role of Carbon Capture and Utilization, Carbon Capture and Storage, and Biomass to Enable a Net-Zero-CO_2 Emissions Chemical Industry. *Ind Eng Chem Res* **2020**, *59* (15), 7033–7045. https://doi.org/10.1021/acs.iecr.9b06579.

(19) Bushuyev, O. S.; de Luna, P.; Dinh, C. T.; Tao, L.; Saur, G.; van de Lagemaat, J.; Kelley, S. O.; Sargent, E. H. What Should We Make with CO_2 and How Can We Make It? *Joule* **2018**, *2* (5), 825–832. https://doi.org/10.1016/j.joule.2017.09.003.

(20) Van Daele, K.; De Mot, B.; Pupo, M.; Daems, N.; Pant, D.; Kortlever, R.; Breugelmans, T. Sn-Based Electrocatalyst Stability: A Crucial Piece to the Puzzle for the Electrochemical CO_2 Reduction toward Formic Acid. *ACS Energy Lett* **2021**, *6* (12), 4317–4327. https://doi.org/10.1021/acsenergylett.1c02049.

(21) Choukroun, D.; Pacquets, L.; Li, C.; Hoekx, S.; Arnouts, S.; Baert, K.; Hauffman, T.; Bals, S.; Breugelmans, T. Mapping Composition–Selectivity Relationships of Supported Sub-10 Nm Cu–Ag Nanocrystals for High-Rate CO_2 Electroreduction. *ACS Nano* **2021**, acsnano.1c04943. https://doi.org/10.1021/acsnano.1c04943.

(22) Wang, Q.; Dong, H.; Yu, H.; Yu, H. Enhanced Performance of Gas Diffusion Electrode for Electrochemical Reduction of Carbon Dioxide to Formate by Adding Polytetrafluoroethylene into Catalyst Layer. *J Power Sources* **2015**, *279*, 1–5. https://doi.org/10.1016/j.jpowsour.2014.12.118.

(23) Kopljar, D.; Inan, A.; Vindayer, P.; Wagner, N.; Klemm, E. Electrochemical Reduction of CO_2 to Formate at High Current Density Using Gas Diffusion Electrodes. *J Appl Electrochem* **2014**, *44* (10), 1107–1116. https://doi.org/10.1007/s10800-014-0731-x.

(24) Chen, C.; Khosrowabadi Kotyk, J. F.; Sheehan, S. W. Progress toward Commercial Application of Electrochemical Carbon Dioxide Reduction. *Chem* **2018**, *4* (11), 2571–2586. https://doi.org/10.1016/j.chempr.2018.08.019.

(25) Merino-Garcia, I.; Tinat, L.; Albo, J.; Alvarez-Guerra, M.; Irabien, A.; Durupthy, O.; Vivier, V.; Sánchez-Sánchez, C. M. Continuous Electroconversion of CO_2 into Formate Using 2 Nm Tin Oxide Nanoparticles. *Appl Catal B* **2021**, *297*, 120447. https://doi.org/10.1016/j.apcatb.2021.120447.

(26) Chen, P.; Jiao, Y.; Zhu, Y.-H.; Chen, S.-M.; Song, L.; Jaroniec, M.; Zheng, Y.; Qiao, S.-Z. Syngas Production from Electrocatalytic CO_2 Reduction with High Energetic Efficiency and Current Density. *J Mater Chem A Mater* **2019**, *7* (13), 7675–7682. https://doi.org/10.1039/C9TA01932D.

(27) Brandl, P.; Bui, M.; Hallett, J. P.; Mac Dowell, N. Beyond 90% Capture: Possible, but at What Cost? *International Journal of Greenhouse Gas Control* **2021**, *105*, 103239. https://doi.org/10.1016/j.ijggc.2020.103239.

(28) Sullivan, I.; Goryachev, A.; Digdaya, I. A.; Li, X.; Atwater, H. A.; Vermaas, D. A.; Xiang, C. Coupling Electrochemical CO_2 Conversion with CO_2 Capture. *Nat Catal* **2021**, *4* (11), 952–958. https://doi.org/10.1038/s41929-021-00699-7.

(29) Gutiérrez-Sánchez, O.; Bohlen, B.; Daems, N.; Bulut, M.; Pant, D.; Breugelmans, T. A State-of-the-Art Update on Integrated CO_2 Capture and Electrochemical Conversion Systems. *ChemElectroChem* **2022**, *9* (5), e20210154. https://doi.org/10.1002/celc.202101540.

(30) Li, M.; Irtem, E.; Iglesias van Montfort, H.-P.; Abdinejad, M.; Burdyny, T. Energy Comparison of Sequential and Integrated CO_2 Capture and Electrochemical Conversion. *Nat Commun* **2022**, *13* (1), 5398. https://doi.org/10.1038/s41467-022-33145-8.

(31) Noda, H.; Ikeda, S.; Oda, Y.; Imai, K.; Maeda, M.; Ito, K. Electrochemical Reduction of Carbon Dioxide at Various Metal Electrodes in Aqueous Potassium Hydrogen Carbonate Solution. *Bull Chem Soc Jpn* **1990**, *63* (9), 2459–2462. https://doi.org/10.1246/bcsj.63.2459.

(32) Gutiérrez-Sánchez, O.; Daems, N.; Offermans, W.; Birdja, Y. Y.; Bulut, M.; Pant, D.; Breugelmans, T. The Inhibition of the Proton Donor Ability of Bicarbonate Promotes the Electrochemical Conversion of CO_2 in Bicarbonate Solutions. *Journal of CO_2 Utilization* **2021**, *48*, 101521. https://doi.org/10.1016/j.jcou.2021.101521.

(33) Hori, Y.; Suzuki, S. Electrolytic Reduction of Bicarbonate Ion at a Mercury Electrode. *J Electrochem Soc* **1983**, *130* (12), 2387–2390. https://doi.org/10.1149/1.2119593.

(34) Dunwell, M.; Lu, Q.; Heyes, J. M.; Rosen, J.; Chen, J. G.; Yan, Y.; Jiao, F.; Xu, B. The Central Role of Bicarbonate in the Electrochemical Reduction of Carbon Dioxide on Gold. *J Am Chem Soc* **2017**, *139* (10), 3774–3783. https://doi.org/10.1021/jacs.6b13287.

(35) Gutiérrez-Sánchez, O.; Daems, N.; Bulut, M.; Pant, D.; Breugelmans, T. Effects of Benzyl-Functionalized Cationic Surfactants on the Inhibition of the Hydrogen Evolution Reaction in CO_2 Reduction Systems. *ACS Appl Mater Interfaces* **2021**, *13* (47), 56205–56216. https://doi.org/10.1021/acsami.1c17303.

(36) Li, T.; Lees, E. W.; Goldman, M.; Salvatore, D. A.; Weekes, D. M.; Berlinguette, C. P. Electrolytic Conversion of Bicarbonate into CO in a Flow Cell. *Joule* **2019**, *3* (6), 1487–1497. https://doi.org/10.1016/j.joule.2019.05.021.

(37) Li, T.; Lees, E. W.; Zhang, Z.; Berlinguette, C. P. Conversion of Bicarbonate to Formate in an Electrochemical Flow Reactor. *ACS Energy Lett* **2020**, *5* (8), 2624–2630. https://doi.org/10.1021/acsenergylett.0c01291.

(38) Lees, E. W.; Goldman, M.; Fink, A. G.; Dvorak, D. J.; Salvatore, D. A.; Zhang, Z.; Loo, N. W. X.; Berlinguette, C. P. Electrodes Designed for Converting Bicarbonate into CO. *ACS Energy Lett* **2020**, 2165–2173. https://doi.org/10.1021/acsenergylett.0c00898.

(39) Gutiérrez-Sánchez, O.; de Mot, B.; Bulut, M.; Pant, D.; Breugelmans, T. Engineering Aspects for the Design of a Bicarbonate Zero-Gap Flow Electrolyzer for the Conversion of CO_2 to Formate. *ACS Appl Mater Interfaces* **2022**, *14* (27), 30760–30771. https://doi.org/10.1021/acsami.2c05457.

(40) de Mot, B.; Hereijgers, J.; Daems, N.; Breugelmans, T. Insight in the Behavior of Bipolar Membrane Equipped Carbon Dioxide Electrolyzers at Low Electrolyte Flowrates.

Chemical Engineering Journal **2022**, *428*, 131170. https://doi.org/10.1016/j.cej.2021.131170.

(41) Blommaert, M. A.; Aili, D.; Tufa, R. A.; Li, Q.; Smith, W. A.; Vermaas, D. A. Insights and Challenges for Applying Bipolar Membranes in Advanced Electrochemical Energy Systems. *ACS Energy Lett* **2021**, *6* (7), 2539–2548. https://doi.org/10.1021/acsenergylett.1c00618.

(42) Chuah, C. Y.; Kim, K.; Lee, J.; Koh, D.-Y.; Bae, T.-H. CO_2 Absorption Using Membrane Contactors: Recent Progress and Future Perspective. *Ind Eng Chem Res* **2020**, *59* (15), 6773–6794. https://doi.org/10.1021/acs.iecr.9b05439.

(43) Gutierrez-Sanchez, O.; De Mot, B.; Bulut, M.; Pant, D.; Breugelmans, T. Engineering Aspects for the Design of a Bicarbonate Zero-Gap Flow Electrolyzer for the Conversion of CO_2 to Formate. *ACS Appl Mater Interfaces* **2022**, *14* (27), 30760-30771. https://doi.org/10.1021/acsami.2c05457.

(44) Franzen, D.; Ellendorff, B.; Paulisch, M. C.; Hilger, A.; Osenberg, M.; Manke, I.; Turek, T. Influence of Binder Content in Silver-Based Gas Diffusion Electrodes on Pore System and Electrochemical Performance. *J Appl Electrochem* **2019**, *49* (7), 705–713. https://doi.org/10.1007/s10800-019-01311-4.

(45) de Mot, B.; Ramdin, M.; Hereijgers, J.; Vlugt, T. J. H.; Breugelmans, T. Direct Water Injection in Catholyte-Free Zero-Gap Carbon Dioxide Electrolyzers. *ChemElectroChem* **2020**, *7* (18), 3839–3843. https://doi.org/10.1002/celc.202000961.

(46) Joshi, S.; Kalyanasundaram, S.; Balasubramanian, V. Quantitative Analysis of Sodium Carbonate and Sodium Bicarbonate in Solid Mixtures Using Fourier Transform Infrared Spectroscopy (FT-IR). *Appl Spectrosc* **2013**, *67* (8), 841–845. https://doi.org/10.1366/12-06915.

(47) Baldassarre, M.; Barth, A. The Carbonate/Bicarbonate System as a PH Indicator for Infrared Spectroscopy. *Analyst* **2014**, *139* (9), 2167. https://doi.org/10.1039/c3an02331a.

(48) Davis, A. R.; Oliver, B. G. A Vibrational-Spectroscopic Study of the Species Present in the CO_2-H_2O System. *J Solution Chem* **1972**, *1* (4), 329–339. https://doi.org/10.1007/BF00715991.

(49) Li, Y. C.; Lee, G.; Yuan, T.; Wang, Y.; Nam, D.-H.; Wang, Z.; García de Arquer, F. P.; Lum, Y.; Dinh, C.-T.; Voznyy, O.; Sargent, E. H. CO_2 Electroreduction from Carbonate

Electrolyte. *ACS Energy Lett* **2019**, *4* (6), 1427–1431. https://doi.org/10.1021/acsenergylett.9b00975.

(50) Chen, L.; Xu, Q.; Oener, S. Z.; Fabrizio, K.; Boettcher, S. W. Design Principles for Water Dissociation Catalysts in High-Performance Bipolar Membranes. *Nat Commun* **2022**, *13* (1), 3846. https://doi.org/10.1038/s41467-022-31429-7.

(51) Bui, J. C.; Corpus, K. R. M.; Bell, A. T.; Weber, A. Z. On the Nature of Field-Enhanced Water Dissociation in Bipolar Membranes. *The Journal of Physical Chemistry C* **2021**, *125* (45), 24974–24987. https://doi.org/10.1021/acs.jpcc.1c08276.

Table of Contents graphic